Performance analysis and insights into Schottky-gate and insulated-gate GaN-on-Si RF switch devices: A comparative study on RF isolation

Yuchen Qian(钱禹辰)[1,2], Jiejie Zhu(祝杰杰)[1,2,†], Mengdi Li(李萌迪)[1,2], Yuxin Cheng(程宇鑫)[1,2], Linjie Qin(秦灵洁)[1,2], Yuxi Zhou(周钰晰)[1,2], Boxuan Gao(高渤轩)[1,2], Bowen Zhang(张博文)[1,2], Yiwei Wang(王艺伟)[1,2], Mingcheng Zhang(张明辰)[1,2], Yichong Ding(丁一翀)[1,2], Mingkai You(游明恺)[3], Wanshuo Liao(廖万硕)[1,2], Shuo Wang(王朔)[1,2], and Xiaohua Ma(马晓华)[1,2]

[1] *National Engineering Research Center of Wide Band-gap Semiconductor, Xi'an* 710071, *China*
[2] *School of Microelectronics, Xidian University, Xi'an* 710071, *China*
[3] *Faculty of Science, National University of Singapore, Singapore* 117542, *Singapore*

(Received 9 September 2025; revised manuscript received 6 November 2025; accepted manuscript online 14 November 2025)

Radio-frequency (RF) switches play a pivotal role in reconfigurable front-ends, antenna tuning, and transmit/receive modules; however, fundamental studies on their device-level physics and switching mechanisms remain relatively limited. This work presents a comparative investigation of Schottky-gate and insulated-gate RF switch devices fabricated on GaN-on-Si substrates, and provides the first systematic evidence of a correlation between drain-induced barrier lowering (DIBL) and isolation in insulated-gate structures. Small-signal characterization further reveals that the insertion loss shows only a small difference between the two devices, whereas the isolation performance differs considerably. To gain further insight into this phenomenon, we conducted an in-depth investigation. Experimental results demonstrate that although the incorporation of a SiN gate dielectric effectively reduces the peak electric field in the AlGaN barrier, this compromise in turn weakens gate controllability and aggravates the DIBL effect. As a result, although the electric field is mitigated, the addition of the gate insulator counterintuitively reduces the breakdown voltage, primarily due to buffer leakage. Benefiting from stronger gate control, the Schottky-gate switch consistently exhibits superior isolation compared with its insulated-gate counterpart, although the disparity diminishes with increasing frequency. At higher frequencies, particularly in millimeter-wave regimes, parasitic effects and fringing capacitance dominate, rendering the isolation difference nearly negligible. These findings not only provide new insights into the device physics of GaN-on-Si RF switches but also offer practical design guidelines for achieving high-performance operation.

Keywords: GaN, radio-frequency (RF) switch, drain-induced barrier lowering (DIBL), isolation

PACS: 61.72.uj, 71.55.Eq, 07.50.Qx, 73.40.Qv

DOI: 10.1088/1674-1056/ae1f7d **CSTR:** 32038.14.CPB.ae1f7d

1. Introduction

With the rapid advancement of modern communication technologies — including mobile phones, base stations, and satellites — both societal and economic efficiency have improved markedly, while interpersonal connectivity has become more seamless. Among the critical components in communication systems, radio-frequency (RF) switches play a central role in controlling signal transmission and reception quality. To meet diverse design and performance requirements, a range of technologies has been explored for RF switch implementation, including microelectromechanical systems (MEMS), PIN diodes, phase-change materials, silicon-on-insulator (SOI), gallium nitride (GaN), and others.[1–6] RF switches based on MEMS materials are easy to fabricate but suffer from low integration density and high sensitivity to environmental influences. SOI-based RF switches exhibit excellent isolation performance, yet their limited power-handling capacity restricts their application scope. GaAs pseudomorphic high-electron-mobility transistor (pHEMT) switches demonstrate outstanding noise performance and are conducive to integration; however, their low power tolerance similarly confines them to narrow application ranges. Among these, GaN-based RF switches have emerged as a highly reliable and competitive option, offering favorable characteristics in terms of performance, integration, and robustness.[7]

Owing to its wide bandgap, strong thermal stability and the ability to form a high-mobility two-dimensional electron gas at the AlGaN/GaN interface, GaN has attracted extensive attention for high-frequency and high-power electronics.[8] Consequently, significant research has been devoted to GaN-based devices such as power amplifiers (PAs) and low-noise amplifiers.[9,10] Another critical component in transmit/receive modules and monolithic microwave integrated circuits (MMICs) is the GaN HEMT-based RF switch.[11–14] However, current RF switch designs are often adapted from existing PA architectures, typically by relocating the gate elec-

†Corresponding author. E-mail: jjzhu@mail.xidian.edu.cn

© 2026 Chinese Physical Society and IOP Publishing Ltd. All rights, including for text and data mining, AI training, and similar technologies, are reserved.

CPB Online First

trode to the center of the device. This approach is suboptimal because the functions of these components differ fundamentally: PAs are designed for signal amplification, whereas the primary role of an RF switch is to control the signal's passage or blockage. As a result, while considerable research effort has focused on PA development — spanning process optimization, modeling and stability design — dedicated research on RF switches has been comparatively overlooked.

In this work, we conducted a comparative study of the key performance parameters of GaN-on-Si RF switch devices featuring Schottky-gate and metal–insulator–semiconductor gate structures. Motivated by the observed discrepancies in signal isolation (ISO) and insertion loss (IL) between the two device types, DC measurements and technology computer-aided design (TCAD) simulations were employed to gain a deeper insight. Our DC characterization revealed significant differences in the breakdown voltage of the devices. Based on these observations, we analyzed the electric field and carrier distributions within the devices, and simultaneously extracted the drain-induced barrier lowering (DIBL) effect. The results indicate that vertical leakage current is the dominant mechanism responsible for the reduced breakdown voltage in the insulated-gate devices. Furthermore, this study establishes a physical connection between DC degradation mechanisms and RF performance metrics. Also, for the first time, we demonstrate the correlation between the DIBL effect and ISO. It was found that the DIBL effect in insulated-gate devices degrades the off-state capacitance, although this discrepancy diminishes at higher signal frequencies due to parasitic effects. These findings underscore the critical roles of gate electrostatic control and buffer leakage in determining the overall performance of GaN-based RF switches. Based on these insights, we propose practical guidelines for selecting gate architectures and buffer design strategies for RF switches optimized for various frequency bands.

2. Devices structure and fabrication

In this paper, the GaN-on-Si RF switches with Schottky-gate and insulated-gate structures were fabricated using the same process flow as reported in our previous work.[15] A three-dimensional schematic of the device structure is shown in Fig. 1. The devices were grown on a high-resistivity silicon substrate. From bottom to top, the epitaxial layers were deposited using metal–organic chemical vapor deposition and consisted of a carbon-doped GaN buffer, a 150 nm unintentionally doped GaN layer, a 1 nm AlN interlayer, a 7 nm AlGaN barrier layer, and a 1 nm GaN cap layer.

To enhance the sheet carrier density and reduce the sheet resistance of the heterostructure, a 120 nm low-pressure chemical vapor deposition (LPCVD) high-stress passivation layer was applied. This reduction in sheet resistance helped to lower the on-resistance (R_{on}) of the device, thereby improving the IL performance of the RF switch.[16] Ohmic contacts were realized using regrown n^+ InGaN, and the ohmic metal consisted of Ti/Au.[17] For both type A and type B devices, the gate stack comprised Ni/Au/Ti; the distinction lies in the gate architecture. Type A employed a Schottky gate in which Ni directly contacts the semiconductor, while type B used an insulated-gate structure with a 5 nm SiN layer deposited by plasma-enhanced atomic layer deposition (PEALD) inserted between the gate metal and the semiconductor.

A gate resistor of 4.2 kΩ was externally connected, leveraging the channel resistance between the AlGaN/GaN interface to avoid the fabrication challenges associated with sputtered metal resistors. The inclusion of this series gate resistor serves to suppress signal leakage through the gate. The fabricated devices featured a 2 μm spacing between the two signal ports (functionally equivalent to the conventional source-to-drain distance, L_{sd}), with a gate length (L_g) of 0.25 μm centrally located between them, and a total gate width of 1×75 μm.

Based on the fabricated devices, both DC and RF characterizations were performed to analyze and compare the performance differences between the Schottky-gate and insulated-gate RF switches.

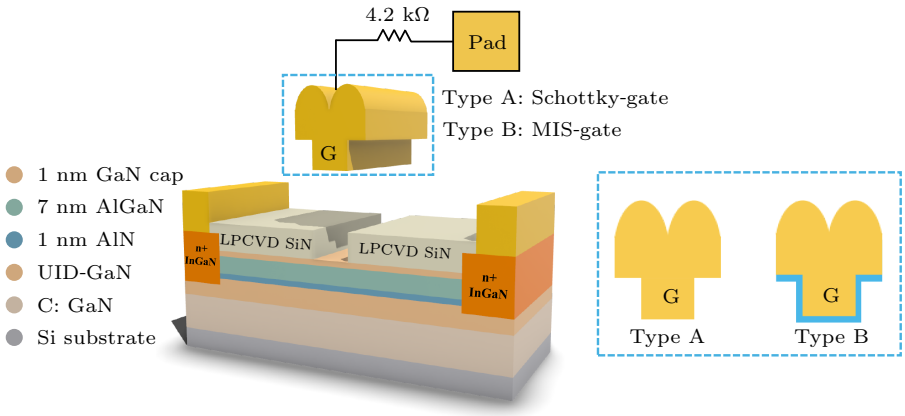


Fig. 1. Three-dimensional structure of GaN-on-Si RF switch and gate design (LPCVD, low-pressure chemical vapor deposition; MIS, metal–insulator–semiconductor; UID, unintenionally doped).

CPB Online In-Press

3. Results and discussion

An RF switch governs the conduction and isolation of high-frequency signals, which defines its two distinct operating states: the on-state and the off-state. In the on-state, the impedance should be sufficiently low to allow the signal to pass through with minimal loss, ensuring signal integrity without distortion. In the off-state, the impedance should be sufficiently high to prevent signal leakage. To more accurately evaluate the performance of RF switch devices, the following equations are used:[18]

$$\mathrm{FOM} = R_{\mathrm{on}} \times C_{\mathrm{off}}, \tag{1}$$

where

$$\begin{aligned} R_{\mathrm{on}} &= 2Z_0\left(10^{-\frac{S_{21}(\mathrm{dB})}{20}} - 1\right), \\ C_{\mathrm{off}} &= \frac{1}{2Z_0\omega\sqrt{10^{-\frac{S_{21}(\mathrm{dB})}{10}} - 1}}. \end{aligned} \tag{2}$$

The on- and off-state RF performances of the switch can be quantitatively assessed through the scattering parameter S_{21}, which directly reflects the transmission characteristics of the device. In the on-state, a lower IL — corresponding to a higher $|S_{21}|$ — is preferred to ensure minimal signal attenuation and distortion. Conversely, in the off-state, a higher isolation — corresponding to a lower $|S_{21}|$ — is desired to suppress signal leakage. The on-resistance (R_{on}) and off-state capacitance (C_{off}) were extracted from the measured S_{21} values using the aforementioned analytical expressions.

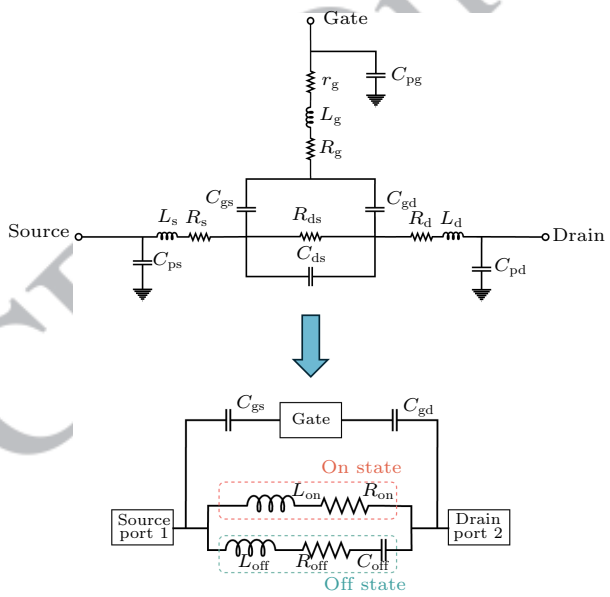


Fig. 2. Full and simplified small-signal equivalent circuit models of an RF switch.

The measured results in Fig. 3 indicate only a small difference in the IL between insulated-gate and Schottky-gate devices, with a slight advantage for insulated-gate structures at low frequencies and a crossover at higher frequencies. The lower gate leakage of insulated-gate RF switches helps suppress signal leakage from the gate. However, since the series gate resistor itself is intended to mitigate gate signal leakage, the improvement is not particularly significant. In contrast, the isolation characteristics show a more intriguing trend. Schottky-gate devices consistently exhibit higher isolation than their insulated-gate counterparts, but the difference gradually decreases with increasing frequency. For example, at 100 MHz, a Schottky-gate switch achieves 4.4 dB higher isolation; this advantage reduces to 2.6 dB at 3.6 GHz and further decreases to only 0.14 dB at 40 GHz. This phenomenon has not been previously reported; therefore, we attempted to analyze and explain it through DC characterization and TCAD simulations to investigate the underlying mechanisms.

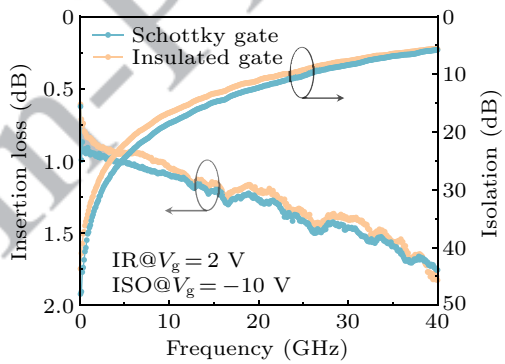


Fig. 3. Frequency dependence of insertion loss and isolation for Schottky-gate and insulated-gate RF switches, obtained from small-signal measurements in the range of 1 MHz–40 GHz at $V_g = 2$ V (IL) and $V_g = -10$ V (ISO).

The DC measurement data were obtained using a Keithley 4200A-SCS semiconductor parameter analyzer, and the results are presented in Figs. 4 and 5. Significant differences were observed between the two types of devices. After the introduction of the gate dielectric, the insulated-gate device exhibited a noticeable negative shift in threshold voltage. Using a drain voltage of $V_d = 10$ V, the threshold voltage was extracted at the point where $I_{ds} = 1$ mA/mm. The Schottky-gate device showed a threshold voltage of -1 V, while the insulated-gate device exhibited a much lower threshold of -4.7 V. In terms of maximum drain current, the Schottky-gate device reached $I_{ds,max} = 1088$ mA/mm, while the insulated-gate device achieved a higher value of 1269 mA/mm.

However, the peak transconductance $G_{m,max}$ of the Schottky-gate device significantly outperformed that of its insulated-gate counterpart. The Schottky-gate device exhibited a peak G_m of 492 mS/mm, whereas the insulated-gate device showed a lower value of 416 mS/mm. Although peak transconductance is a critical figure of merit for GaN-based power amplifiers, since it directly affects cutoff and maximum operating frequencies,[9] it plays a minimal role in the performance of RF switch devices.[16]

Chin. Phys. B Online In-Press

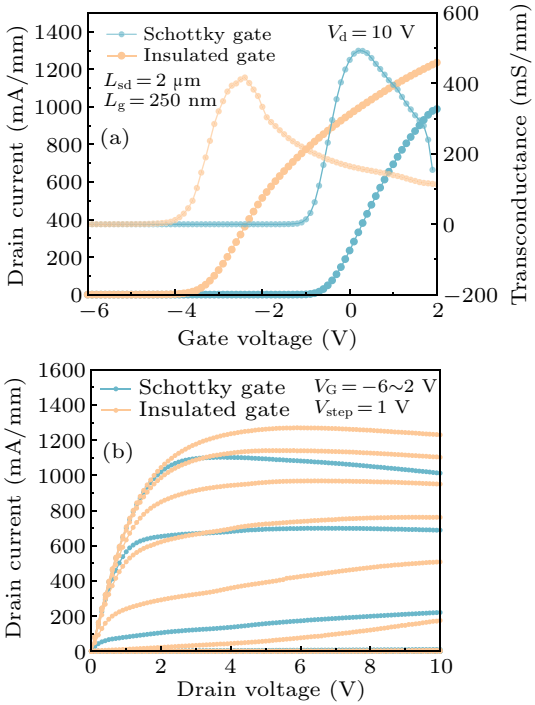


Fig. 4. (a) Transfer and (b) output characteristics of GaN-on-Si RF switch devices. Blue curves represent Schottky-gate devices while yellow curves correspond to insulated-gate devices.

Surprisingly, despite the widespread approach of enhancing breakdown performance by introducing high-quality gate dielectrics, our results indicate otherwise. The fabricated insulated-gate RF switch exhibited a breakdown voltage of only 25 V, whereas the Schottky-gate device counterpart achieved more than twice that value, reaching 58 V. The breakdown is not irreversible, suggesting that it is predominantly governed by leakage conduction rather than catastrophic damage. The insulated-gate device exhibited a lower gate leakage current than the Schottky-gate device. This significant suppression of leakage is attributed to the high quality of the PEALD-grown SiN dielectric. However, these improvements did not translate into enhanced breakdown capability.

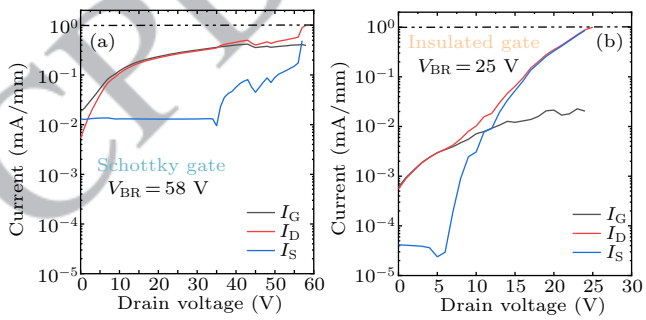


Fig. 5. Off-state breakdown characteristics of GaN-on-Si RF switch devices: (a) Schottky-gate structure and (b) insulated-gate structure.

Breakdown in GaN HEMT-based devices is generally classified into two categories: one induced by leakage currents and the other triggered by excessive electric fields. In GaN-based devices and RF switches, high electric fields typically concentrate near the gate, more specifically at the gate edge on the drain side.[19] Leakage-induced breakdown, on the other hand, can be further divided into two types: one originating from buffer leakage and the other from gate leakage.[20] To investigate the underlying mechanisms, we performed device simulations using Silvaco TCAD to analyze the electric field distribution and carrier concentration within the structures.

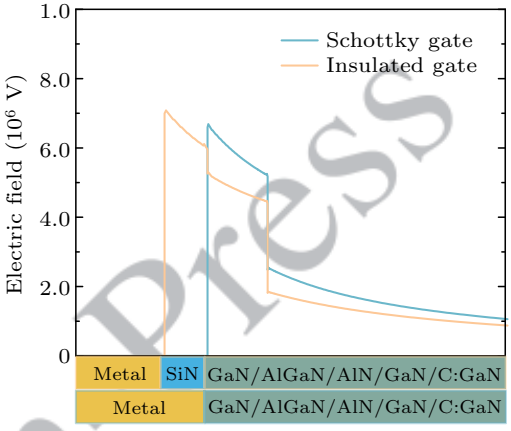


Fig. 6. Comparison of TCAD-simulated electric field distributions for Schottky-gate and insulated-gate devices.

The dielectric constant of SiN is significantly higher than that of AlGaN and GaN, and its critical breakdown field is correspondingly superior. As shown in Fig. 6, TCAD simulations reveal that the introduction of a SiN dielectric layer effectively reduces the peak electric field in the AlGaN barrier.[21] This forms the basis of the widely adopted strategy of employing a SiN insulating layer to enhance device breakdown voltage. However, in our experimental results, the addition of the SiN dielectric layer led to a pronounced reduction in breakdown voltage.

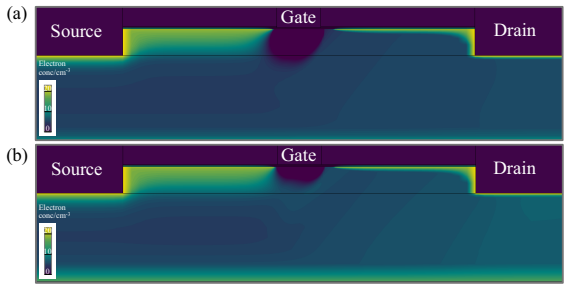


Fig. 7. Electron concentration distribution in a GaN RF switch under the bias conditions of $V_d = 10$ V and $V_g = -6$ V: (a) Schottky-gate device and (b) insulated-gate device. After adopting the insulated-gate, the gate control ability is weakened and the depletion region becomes smaller.

To further investigate this phenomenon, TCAD simulations of the carrier concentration distribution in the off-state were performed, as illustrated in Fig. 7. The results clearly indicate that the Schottky-gate device exhibits stronger gate control than the insulated-gate device. Under identical bias conditions, the depletion region in the Schottky-gate device extends significantly deeper than in the insulated-gate device.

$$\mathrm{DIBL} = \frac{\Delta V_{\mathrm{th}}}{\Delta V_{\mathrm{d}}}. \tag{3}$$

CPB Online In Press

Correlating these findings with the device DIBL characteristics, we extracted the threshold voltage V_{th} at I_d = 1 mA/mm for V_d = 1 V and 10 V, as calculated using Eq. (3). The DIBL values for the insulated-gate and Schottky-gate devices were 166 mV/V and 45 mV/V, respectively. When the threshold voltage was obtained via the tangent-line method, the corresponding DIBL values were 88 mV/V and 44 mV/V, respectively. These results confirm that the insulated-gate device exhibits weaker gate control, with a higher concentration of free electrons in the buffer and more severe vertical leakage.[22,23]

These RF figures of merit, together with key DC parameters, are summarized in Table 1, enabling a direct correlation between static electrical characteristics and high-frequency switching behavior.

Table 1. Comparison of DC and RF performance parameters for insulated-gate and Schottky-gate GaN-on-Si RF switches.

Sample	Insulated gate	Schottky gate
V_{th} [1)] (V)	−4.7/−3.3	−1.0/−0.5
DIBL[2)] (mV/V)	166 / 88	44 / 45
$I_{ds,max}$ (mA/mm)	1269	1088
Max. G_m (mS/mm)	416	492
Off-state breakdown (V)	25	58
ISO @ 3.6/18 GHz (dB)	−24.6/−11.7	−27.2/−13.2
IL @ 3.6/18 GHz (dB)	−0.93/−1.20	−0.97/−1.26
R_{on} @ 3.6/18 GHz (Ω·mm)	0.84/1.11	0.89/1.17
C_{off} @ 3.6/18 GHz (pF/mm)	0.346/0.314	0.257/0.264
FOM @ 3.6/18 GHz (fs)	290.6/348.5	228.7/308.9

1) V_{th} extraction method: the value on the left of the solidus (/) is obtained at I_d = 1 mA/mm, and the value on the right is obtained using the tangent method.

2) DIBL extraction method: the value on the left of the solidus is obtained from the threshold voltage at I_d = 1 mA/mm, and the value on the right is obtained from the threshold voltage using the tangent method.

The introduction of the PEALD-SiN gate dielectric is intended to mitigate gate leakage and reduce the peak electric field in the AlGaN barrier, providing a protective effect. However, this design inherently weakens the gate's control over the channel, leading to insufficient channel modulation. This weaker control aggravates the DIBL effect and, consequently, reduces the breakdown voltage. This presents a critical trade-off: improved gate robustness at the cost of degraded electrostatic control. This dilemma mirrors the classic scaling challenge in MOSFETs, where thinner gate oxides are required to maintain control in shorter channels, highlighting a fundamental compromise between device reliability and performance.

For an RF switch, this weaker gate control directly deteriorates ISO. Under AC conditions, it leads to an increase in off-state capacitance, thereby degrading isolation — an effect particularly evident at relatively low frequencies. At higher frequencies, however, extrinsic factors such as parasitic effects and fringing-field capacitances begin to dominate, rendering the isolation difference between the two device types negligible. These parasitic effects include capacitance, inductance, and resistance, primarily originating from the test pads and interconnect metals. At low frequencies, the impact of these parasitic elements is minimal because their impedance is either extremely high (for parasitic capacitance) or extremely low (for parasitic inductance). As the frequency increases, this situation changes fundamentally: these previously insignificant parasitics start to exhibit substantial impedance, with their influence dominating the actual circuit behavior and even masking the intrinsic characteristics of the device. In this high-frequency, parasitic-dominated regime, overall performance becomes primarily governed by factors such as epitaxial material quality, layout design, and process control. These findings establish a clear link between the device's DC characteristics and its RF transmission/isolation performance, while also identifying the dominant performance-limiting factors across different frequency regimes.

In most cases, RF switches are derived from minor modifications of high-performance PA devices, and research on the root causes of RF switch performance characteristics remains limited. This work demonstrates that, for applications below 18 GHz, optimizing the gate design to improve gate controllability is critical for RF switches. In contrast, at frequencies above 18 GHz, material quality and process control become the dominant determinants of performance. This insight provides valuable guidance for the optimization of GaN-on-Si RF switches.

GaN technology currently encompasses various development paths, including GaN-on-Si, GaN-on-SiC, GaN-on-GaN, GaN-on-sapphire, and GaN-on-SOI. However, the most widely adopted platforms by manufacturers and engineers remain the well-established GaN-on-Si and GaN-on-SiC. GaN-on-SiC, with its superior epitaxial quality, low defect density, and minimal RF loss, has been extensively implemented in circuit designs. Nevertheless, it is often unsuitable for cost-sensitive applications. In contrast, GaN-on-Si benefits from the mature, large-scale, and low-cost silicon substrate technology. While GaN-on-Si power devices have been broadly adopted, RF devices based on this platform have received comparatively limited research attention, leaving significant room for exploration and development in this area.

For GaN-on-Si RF switches, numerous aspects remain to be optimized. A primary concern is the parasitic channel formed between the Si substrate and the AlN nucleation layer, which degrades signal transmission quality — a particularly critical issue for GaN MMICs.[24,25] In contrast, comparatively little attention has been given to the influence of the buffer and gate structures, despite their significant impact on device performance. Our results indicate that DC DIBL behavior and gate controllability are strongly correlated with

CPB Online In-Press

RF isolation capability and off-state capacitance within the 0–18 GHz frequency range. For this regime, improving the DC characteristics and suppressing the DIBL effect can effectively enhance device isolation. Common strategies include increasing the buffer doping concentration,[26,27] introducing an AlGaN back-barrier[28] structure, and applying GaN-on-SOI[11] technology.

4. Conclusion

Research on RF switch devices remains limited, and many underlying mechanisms are still not fully understood. This work compares the DC characteristics, signal transmission, and isolation mechanisms of Schottky-gate and insulated-gate RF switch devices, and provides an in-depth analysis of their interrelations. The introduction of a dielectric layer can reduce the peak electric field in the AlGaN material; however, it also weakens the gate control capability, resulting in a pronounced DIBL effect and, consequently, a lower breakdown voltage despite the dielectric layer. While the two gate structures exhibit negligible differences in signal transmission, their off-state isolation differs significantly. At high frequencies the parasitic effect reduces the isolation difference, whereas at relatively lower frequencies the difference becomes more pronounced. Due to weaker gate control, signals are more prone to leakage — this is the fundamental reason for the performance disparity between insulated-gate and Schottky-gate RF switch devices, in agreement with theoretical expectations. These insights provide guidance for the design and optimization of GaN-on-Si RF switches, particularly for 0–18 GHz applications.

Acknowledgements

This work was supported by the National Natural Science Foundation of China (Grant Nos. 62188102, 62174125, and 62131014) and Fundamental Research Funds for the Central Universities (Grant No. YJSJ25013).

References

[1] Rebeiz G, Entesari K, Reines I, Park S J, El-Tanani M, Grichener A and Brown A 2009 *IEEE Microwave Magazine* **10** 55
[2] Rozbicki A and Brogle J J 2016 *11th European Microwave Integrated Circuits Conference (EuMIC)* pp. 289–292
[3] Leon A, Reig B, Puyal V, Perret E and Podevin F 2018 *48th European Microwave Conference (EuMC)*
[4] Malladi V N K and Miller M 2019 *2019 IEEE 19th Topical Meeting on Silicon Monolithic Integrated Circuits in RF Systems (SiRF)*
[5] Osmanoglu S and Ozbay E 2019 *2019 European Microwave Conference in Central Europe (EuMCE)*
[6] Hughes G R, Werner E A, Moser N A, Walker Jr D E, Ebel J L, Liddy K J, Green A J, Islam A E, Leedy K D, Schuette M L, *et al*. 2020 *CS MANTECH Conference*
[7] Koudymov A, Rai S, Adivarahan V, Gaevski M, Yang J, Simin C and Khan M A 2004 *IEEE Microwave & Wireless Components Letters* **14** 560
[8] Streicher I, Leone S, Manz C, Kirste L, Prescher M, Waltereit P, Mikulla M, Quay R and Ambacher O 2023 *Crystal Growth & Design* **23** 782
[9] Qin L, Zhu J, Zhu Q, Zhang B, Yuan D, Zhou Y, Li M, Li H, Huang S and Gao B2025 *IEEE Transactions on Electron Devices* **72** 4049
[10] Moyer H P, Kurdoghlian A, Micovic M, Lee T, Hiramoto R O, Be Zaire M J, Nguyen S, Hashimoto P, Schmitz A and Milosavljevic I 2008 *2008 IEEE Compound Semiconductor Integrated Circuits Symposium (CSICS)* 1
[11] Then H W, Koirala P, Varghese L, Zubair A, Bader S, Beumer M, Vora, Golani P, Peck J and Hoff T2024 *IEEE International Electron Devices Meeting (IEDM)*
[12] Lucci L, Charlet I, Gobil Y, Morisot F, Delprato J, Ruel S, Benotmane C, Laulagnet F, Dezest P and Bon R 2024 *IEEE International Electron Devices Meeting (IEDM)*
[13] Micovic M, Kurdoghlian A, Moyer P H, Hashimoto P and Schmitz A 2004 *International Microwave Symposium Digest* 1653
[14] Erturk V, Gurdal A and Ozbay E 2023 *IEEE Microwave and Wireless Technology Letters* **33** 1207
[15] Li M, Zhu J, Qin J, Zhou Y, Zhang B, Zhang M, Su Q, Zhao Z, Zhu Q, Ma X H, et al. 2025 *IEEE Transactions on Electron Devices* **72** 3469
[16] Howell R S, Stewart E J, Freitag R, Parke J, Nechay B, King M, Gupta S, Snook M, Wathuthanthri I, Ralston P, *et al*. 2016 *IEEE MTT-S International Microwave Symposium (IMS)* 1
[17] Zhou Y X, Zhu J, Zhang B, Wang Q, Qin L, Wei L, Li M, Chen B, Zhang M and Hao Y 2025 *IEEE Electron Device Letters* **46** 549
[18] Drozdovski N V and Caverly R H 2002 *IEEE Transactions on Microwave Theory & Techniques* **50** 4
[19] Si J, Wei J, Chen W and Zhang B 2013 *IEEE Transactions on Electron Devices* **60** 3223
[20] Zhao S L, Hou B, Chen W W, Mi M H, Zheng J X, Zhang J C, Ma X H and Hao Y2016 *IEEE Transactions on Power Electronics* **31** 1517
[21] Langpoklakpam C, Kumar H C, Hsieh Y C, Chang E Y and Lee C H 2024 *Solid-State Electronics* **216** 108930
[22] Hult B, Bergsten J, Castillo F D D, Darakchieva V, Malmros A, Hjelmgren H, Thorsell H and Rorsman N 2024 *IEEE Transactions on Electron Devices* **71** 7383
[23] Borga M, Meneghini M, Benazzi D, Canato E and Zanoni E 2019 *Microelectronics Reliability* **100–101** 113461
[24] Liu S and Zhuang Y 2024 *Appl. Phys. Lett.* **125** 023504
[25] Chandrasekar H 2020 *Substrate Effects in GaN-on-Silicon RF Device Technology*
[26] Uren M J and Kuball M 2021 *Jpn. J. Appl. Phys.* **60** SB0802
[27] Choi F S, Griffiths J T, Ren C, Lee K B and Wallis D J 2018 *J. Appl. Phys.* **124** 055702
[28] Medjdoub F and Zegaoui M 2011 *Appl. Phys. Express* **4** 124101

CPB Online IOPPress